Comparison of Isomerization Rates of the Metal Carbonyl Cluster $Cp^*IrCp_2Co_2(CO)_3$ in Three Oxidation States (47e, 48e, 49e): Dramatic Rate Enhancements in the Odd-Electron Species†

William E. Geiger,*,‡ Michael J. Shaw,‡ Martin Wünsch,‡ Craig E. Barnes,*,§ and Frank Holger Foersterling§

Contribution from the Departments of Chemistry, University of Vermont, Burlington, Vermont 05405, and University of Tennessee, Knoxville, Tennessee 37996

Received October 4, 1996⊗

Abstract: The 48-electron cluster $Cp^*IrCp_2Co_2(CO)_3$ has two known isomers, one with a terminal carbonyl ligand and two edge-bridging carbonyls (**1**) and the other with three edge-bridging carbonyls (**2**). The rate of their interconversion is dramatically dependent on the number of electrons in the cluster. NMR studies establish that **2** is the thermodynamically favored isomer and that the isomerization is slow at ambient temperatures in the 48 e^- complex ($k_{isom} \approx 10^{-6}$ s^{-1} at 298 K). In contrast, isomerization proceeds very rapidly ($k_{isom} = 400$ s^{-1}) through the 47-electron monocation as part of an efficient electron-transfer-catalyzed process. Cyclic voltammetry and square-wave voltammetry were used to measure the isomerization rate of the monocation. The catalytic nature of the anodically-induced isomerization was diagnosed by theoretical modeling of the electrode responses and by infrared spectroelectrochemistry using a fiber-optic probe of an electrolysis solution. Reductions of the cluster isomers give 49-electron monoanions. The anion $\mathbf{1}^-$ isomerizes over the period of a bulk electrolysis to $\mathbf{2}^-$, setting the limits of k_{isom} between 10^{-1} and 10^{-3} s^{-1} for $\mathbf{1}^-$. The relative rate of the cluster isomerization increases, therefore, in the order 48 $e^- \ll 49$ $e^- \ll 47$ e^-, with relative rates of $1{:}\approx 10^4{:}10^8$. Rate enhancements are rationalized in terms of changes in occupancies involving redox orbitals either bonding or antibonding with respect to the trimetallic framework. The results constitute a rare example of the determination of a reaction rate through *three* oxidation states of a complex.

Introduction

It is well-known that the reactivity of an organometallic compound may be highly dependent on its electron count (in this context its overall "oxidation state").[1] Although many electron-transfer series have been established,[2,3] the effect of electron transfer on a single reaction rate has generally not been followed through more than two oxidation states.[4,5] Here we report on dramatic changes in the isomerization rate of a metal carbonyl cluster through *three* oxidation states. The results are best understood in terms of the weakening of the metallic framework when the cluster has an electron count other than the electron-precise value[6] of 48 e^- for a trimetallic cluster.

Besides being of fundamental interest, these results are also relevant to the question of the favored bonding modes of carbon monoxide on metal surfaces.[7] The cluster/surface analogy may be particularly significant for chemisorbed CO on metals.[8] If so, the bonding modes of metal carbonyl clusters in different oxidation states may guide our understanding of the way in which metal−adsorbate surface structures depend on the applied potential. The latter is important not only because adsorbed CO may be oxidized on Rh and Ir electrodes,[9] but also because CO is an anodic poison to organic fuels (methanol, etc.) which employ noble metal electrodes.[10]

Approached by different synthetic routes, the cluster $Cp^*IrCp_2Co_2(CO)_3$ may be isolated as two isomers differing in the disposition of their CO groups within the trinuclear core. Isomer **1** has a terminal CO on Ir and two doubly-bridging carbonyls on the dicobalt edge.[11] Isomer **2** has three doubly-bridging carbonyls symmetrically disposed around the triangular framework.[12] The present work shows that **2** is the thermodynami-

† Structural Consequences of Electron-Transfer Reactions Part 33. Part 32: Chin, T. T.; Geiger, W. E.; Rheingold, A. L. *J. Am. Chem. Soc.* **1996**, *118*, 5002.

‡ University of Vermont.

§ University of Tennessee.

⊗ Abstract published in *Advance ACS Abstracts,* March 1, 1997.

(1) Trogler, W. C., Ed. *Organometallic Radical Processes*; Elsevier: Amsterdam, 1990.

(2) (a) Connelly, N. G.; Geiger, W. E. *Advances in Organometallic Chemistry*; Academic Press: New York, 1984; Vol. 23, p 2. (b) Geiger, W. E.; Connelly, N. G. *Advances in Organometallic Chemistry*; Academic Press: New York, 1985; Vol. 24, p 87.

(3) Astruc, D. *Electron Transfer and Radical Processes in Transition Metal Chemistry*; VCH Publishers: New York, 1995.

(4) For example, some noteworthy determinations of rate differences in adjacent oxidation states of mononuclear organometallic compounds follow: (a) metal−alkyl cleavage: Pedersen, A.; Tilset, M. *Organometallics* **1993**, *12*, 56. (b) Migratory insertion: Magnuson, R. H.; Meirowitz, R.; Zulu, S.; Giering, W. P. *J. Am. Chem. Soc.* **1982**, *104*, 5790. (c) Ligand exchange: Zizelman, P. M.; Amatore, C.; Kochi, J. K. *J. Am. Chem. Soc.* **1984**, *106*, 3771.

(5) Ligand exchange in clusters: (a) Arewgoda, M.; Robinson, B. H.; Simpson, J. *J. Am. Chem. Soc.* **1983**, *105*, 1893. (b) Downard, A. J. Robinson, B. H.; Simpson, J. *Organometallics* **1986**, *5*, 1140 and references therein.

(6) Crabtree, R. H. *The Organometallic Chemistry of the Transition Metals*, 2nd ed.; John Wiley and Sons: New York, 1994; p 337 ff.

(7) Yau, S-L.; Gao, X.; Chang, S-C.; Schardt, B. C.; Weaver, M. J. *J. Am. Chem. Soc.* **1991**, *113*, 6049.

(8) Muetterties, E. L. *Chem. Rev.* **1979**, *79*, 91.

(9) Watanabe, M.; Motoo, S. *J. Electroanal. Chem.* **1986**, *202*, 125 and references therein.

(10) Parsons, R.; VanderNoot, T. *J. Electroanal. Chem.* **1988**, *257*, 9.

(11) Herrmann, W. A.; Barnes, C. E.; Zahn, T.; Ziegler, M. L. *Organometallics* **1985**, *4*, 172.

(12) Hörlein, R.; Herrmann, W. A.; Barnes, C. E.; Weber, C.; Krüger, C.; Ziegler, M. L.; Zahn, T. *J. Organomet. Chem.* **1987**, *321*, 257.

S0002-7863(96)03476-2 CCC: $14.00

cally-favored isomer and that the isomerization of **1** to **2** is very slow in the neutral 48 e⁻ clusters.

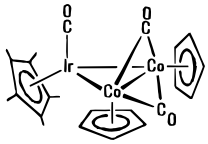

1

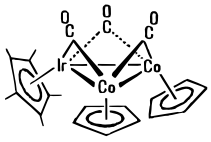

2

The two isomers of $Cp^*IrCp_2Co_2(CO)_3$ are analogous to those known for $Cp_3Rh_3(CO)_3$, namely C_s-$Cp_3Rh_3(CO)(\mu\text{-}CO)_2$ (**3**) and C_{3v}-$Cp_3Rh_3(\mu\text{-}CO)_3$ (**4**).[13,14] We previously reported that isomerization of **3** to **4** was possible through an anodically-initiated electron-transfer catalysis (ETC), but that the isomerization rate constant was too fast to measure.[15] Oxidative initiation of an ETC isomerization process[16] is also found for **1** → **2** in the present study. In this case, however, the isomerization rate (of the 47 e⁻ monocation $\mathbf{1}^+$) is measured by voltammetry and compared to the rate of thermal rearrangement (measured by NMR) for the 48 e⁻ compounds.

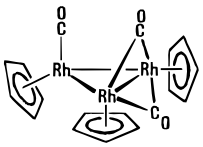

3

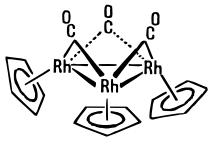

4

Furthermore, the one-electron *reduction* of **1** also gives the all-bridging isomer (as the monoanion $\mathbf{2}^-$), and an estimate of the rate of isomerization of the 49e anion $\mathbf{1}^-$ is possible from voltammetry and coulometry experiments. The finding that the isomerization rate increases in the order $\mathbf{1} \ll \mathbf{1}^- \ll \mathbf{1}^+$ suggests that the rate-limiting step involves elongation of a metal−metal bond in the cluster (*vide infra*).

The flexible nature of the series of complexes $Cp_3M_3(CO)_3$ (M = Co, Rh, Ir) has received a good deal of attention[17,18] and was the subject of a recent theoretical and structural study.[19] The present paper contributes to our understanding of the isomeric preferences and interconversions in this fascinating group of compounds.

Experimental Section

All operations were conducted under an atmosphere of N_2 using standard methodologies. Solvents were dried, distilled, and degassed for synthetic procedures. Electrochemical solvents were prepared as described earlier.[20]

Chemicals. Complexes **1**[11] and **2**[12] were prepared as previously described and checked for isomeric content by ^{1}H-NMR spectroscopy.

Electrochemistry. Voltammetric measurements were obtained on samples housed in a drybox under N_2 using previously-described procedures.[21] The Princetion Applied Research (PARC) 173/276 potentiostat was interfaced through a GPIB to a personal computer. The cyclic and square-wave voltammograms were measured using Quickbasic programs modeled on examples given in the operating manual for the PARC Model 273 potentiostat.[22]

Various reference electrodes, including SCE and Ag/AgCl, were used in this study. All potentials, however, are referenced to that of the ferrocene/ferrocenium couple, obtained experimentally by adding ferrocene as an internal standard at the end of an experiment. Reported potentials may be converted to the SCE scale by addition of 0.46 V in the case of CH_2Cl_2 solutions and 0.56 V in the case of THF. The supporting electrolyte was 0.1 M $[NBu_4][PF_6]$. Electrodes were pretreated by polishing them with a series of diamond pastes. Digital simulations were carried out on a personal computer using DIGISIM (Bioanalytical Systems)[23] for cyclic voltammograms and a program obtained through the internet for square-wave voltammograms.[24] Experimental $E_{1/2}$ values were calculated from the average of the cathodic and anodic peak potentials for a chemically reversible couple.

Spectroscopy. IR spectra were obtained on $CH_2Cl_2/[NBu_4][PF_6]$ solutions of **1** (1.0 mM) before and after anodic electrolysis in a standard three-compartment cell by using the fiber-optic "dip" probe recently described[25] to monitor the working electrode compartment. Spectra were collected on a Matson Polaris FTIR spectrometer operating at 2-cm^{-1} resolution. ESR spectra were obtained using a modified Varian E-4 spectrometer equipped with a frequency counter. DPPH was used to check *g* values. The ESR spectrum of $\mathbf{2}^-$ was obtained by reduction of **1** in Me-THF by a potassium mirror under high vacuum. After brief contact, the solution was poured away from the metal into a sidearm kept cold.

^{1}H NMR spectroscopy was used to monitor the interconversion of **1** and **2** in a thermostated probe at 400 MHz. Samples of either **1** or **2** and solvent were flame-sealed in NMR tubes either under vacuum or in a nitrogen atmosphere.[26]

Results

Oxidation of 1 and 2. When solutions of **1** are investigated at low CV scan rates in THF or CH_2Cl_2 an anodic wave of approximate one-electron height is observed (wave B, Figure 1). The cathodic wave coupled to wave B in the return scan allows an estimate of $E_{1/2} = -0.30$ V for this couple. As will be shown below, wave B arises from the oxidation of isomer **2** ($E^{\mathbf{2}}_{1/2} = -0.30$ V) formed electrocatalytically from **1** during the CV sweep. Two features of Figure 1 deserve further attention: (1) as the scan rate, ν, is increased, a small "prewave" (wave A) appears arising from the oxidation of isomer **1** ($E^{\mathbf{1}}_{1/2} = -0.44$ V, determined through experiments described later); and (2) wave B is not fully chemically reversible, implying that the monocation $\mathbf{2}^+$ partially decomposes over the time scale of the scan at ambient temperatures. Two reactions of the monocations must be considered, therefore, in accounting for the voltammetric data: fast isomerization of $\mathbf{1}^+$ to $\mathbf{2}^+$, and slow decomposition of $\mathbf{2}^+$. It will be shown below that the isomerization of $\mathbf{1}^+$ is about a thousandfold faster than the decomposition of $\mathbf{2}^+$.

Electron-Transfer-Catalyzed (ETC) Isomerization of 1 to 2. Equations 1−4 and Scheme 1 give the reactions involved

(13) (a) Paulus, E. F.; Fischer, E. O.; Fritz, H. P.; Schuster-Woldan, H. *J. Organometal. Chem.* **1967**, *10*, P3. (b) Mills, O. S.; Paulus, E. F. **1967**, *10*, 331. (c) Paulus, E. F. *Acta Crystallogr.* **1969**, *25B*, 2206.

(14) Faraone, F.; Schiavo, S. L.; Bruno, G.; Piraino, P.; Bombieri, G. *J. Chem. Soc., Dalton Trans.* **1983**, 1813.

(15) (a) Mevs, J. M.; Geiger, W. E. *J. Am. Chem. Soc.* **1989**, *111*, 1922. (b) Mevs, J. M.; Gennett, T.; Geiger, W. E. *Organometallics* **1991**, *10*, 1229.

(16) For leading references to ETC reactions in organometallic chemistry see ref 3, Chapter 6.

(17) Leading references may be found in the following: Wadepohl, H.; Gebert, S. *Coord. Chem. Rev.* **1995**, *143*, 535.

(18) Robben, M. P.; Geiger, W. E.; Rheingold, A. L. *Inorg. Chem.* **1994**, *33*, 5615.

(19) Braga, D.; Grepioni, F.; Wadepohl, H.; Gebert, S.; Calhorda, M. J.; Veiros, L. F. *Organometallics* **1995**, *14*, 5350.

(20) (a) Bowyer, W. J.; Geiger, W. E. *J. Am. Chem. Soc.* **1985**, *107*, 5657. (b) Atwood, C. G.; Geiger, W. E.; Bitterwolf, T. E. *J. Electroanal. Chem.* **1995**, *397*, 279.

(21) Richards, T. C.; Geiger, W. E. *J. Am. Chem. Soc.* **1994**, *116*, 2028.

(22) Copies of this interfacing program are available from WEG upon request.

(23) Rudolph, M.; Reddy, D. P.; Feldberg, S. W. *Anal. Chem.* **1993**, *66*, 589A.

(24) Available from Dr. C. Nervi, Torino, Italy (chpc06.ch.unito.it) at ftp://chpc06.ch.unito.it/pub/msdos/chemistry/esp22.zip.

(25) Shaw, M. J.; Geiger, W. E. *Organometallics* **1996**, *15*, 13.

(26) See, for example: Bergman, R. G.; Buchanan, J. M.; McGhee, W. D.; Periana, R. A.; Seidler, P. F.; Trost, M. K.; Wenzel, T. T. In Wayda, A. L.; Darensbourg, M. Y., Eds. *Experimental Organometallic Chemistry*; ACS Symp. Ser. No. 357; American Chemical Society: Washington, DC, 1987; p 227 ff.

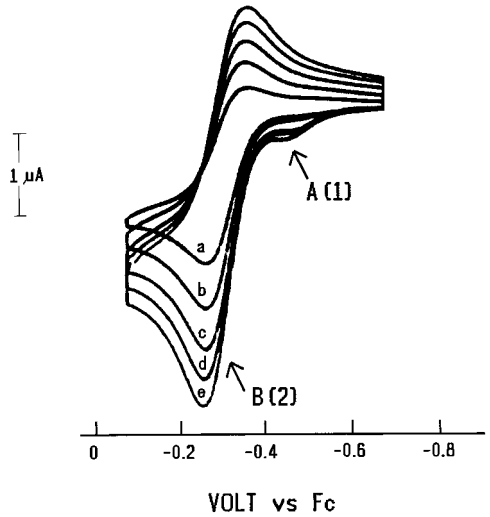

Figure 1. Cyclic voltammetry scans of 0.5 mM **1** in THF (ambient temperature, Pt electrode) at the sweep rates (a) 0.10, (b) 0.20, (c) 0.30, (d) 0.40, and (e) 0.50 V/s.

in the anodic reactions of the clusters. Equations 1−3 constitute an ECE electrocatalytic mechanism if (i) the interconversion between the monocations (eq 2) is rapid and (ii) $E^{\mathbf{2}}_{1/2} > E^{\mathbf{1}}_{1/2}$ (i.e., the oxidation of **2** must be positive of that of **1**). If inequality (ii) were reversed, oxidation of **1** would give $\mathbf{2}^+$ rather than **2** and the oxidation would be stoichiometric (1 faraday/equiv) rather than catalytic in the number of electrons released[27] [such a situation is found in the *reduction* of **1** to give $\mathbf{2}^-$ (see below)]. A simplifying aspect of this system is that the isomerization between the neutral clusters **1** and **2** is sufficiently slow to be ignored in voltammetry scans.

$$\mathbf{1} \rightleftharpoons \mathbf{1}^+ + e^- \qquad E^{1}_{1/2} \tag{1}$$

$$\mathbf{1}^+ \overset{k^+_f}{\rightleftharpoons} \mathbf{2}^+ \qquad K^+_{eq} = k^+_f/k^+_b = [\mathbf{2}^+]/[\mathbf{1}^+] \tag{2}$$

$$\mathbf{2}^+ + e^- \rightleftharpoons \mathbf{2} \qquad E^{2}_{1/2} \tag{3}$$

$$\mathbf{2}^+ \xrightarrow{k_c} \text{fragmentation products} \tag{4}$$

Catalytic Isomerization Demonstrated for Entire Solutions of 1. That isomerization of **1** to **2** occurs through an oxidative ETC mechanism was established by two experiments relying on initiation (eq 1) by either a chemical oxidant or an electrode. In the former case, addition of 0.07 equiv of Cp_2Fe^+ to a CH_2Cl_2 solution of **1** resulted in rapid quantitative formation of **2**, as monitored by IR spectroscopy (ν_{CO} region) and voltammetry [reduction waves for $\mathbf{1}/\mathbf{1}^-$ and $\mathbf{2}/\mathbf{2}^-$ (*vide infra*)]. For the latter, exposure of a CH_2Cl_2/0.1 M $[NBu_4][PF_6]$ solution of **1** to a Pt basket with $E_{appl} = -0.6$ V gave the same rapid conversion to **2** despite the applied potential being significantly *negative* of the $E_{1/2}$ for the oxidation of either isomer. Only about 0.03 faraday/equiv was released in achieving almost complete conversion from **1** to **2**. Figure 2 displays the pertinent IR spectra obtained with a fiber-optic "dip" probe.[25] The fiber-optic method allows IR sampling of the same bulk solution on which voltammetric scans are recorded, an advantage of particular importance for a system such as the present one in which the chemical environment (e.g., trace oxidants) might have a significant effect on the makeup of the solution.

(27) The effect of the relative $E_{1/2}$ values on ETC has been discussed, see Amatore, C. in ref 1, pp 31−34.

Scheme 1

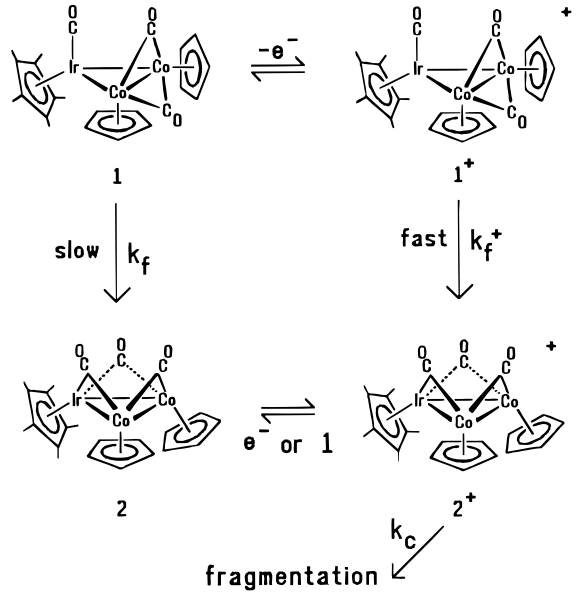

The spectra in Figure 2 show that isomer **2** (ν_{CO} = 1810, 1760 cm^{-1}) replaced approximately 80% of isomer **1** (1940, 1790 cm^{-1}) after passage of just 3% of an electron equivalent. This experiment established that efficient catalytic isomerization occurs *in the bulk of solution*. Slow linear scan voltammograms (LSV) of the oxidation waves of **1** and **2**, by contrast, do not reveal the extent of the isomerization in solution. Except for a small change in the height of the "prewave" A (isomer **1**), the LSVs remain unchanged because the concentrations of **1** and **2** are affected *at the electrode surface* by imposition of the scanning potential. This alteration of isomer concentrations by the small working electrode is useful for measurement of the isomerization rate in the 47 e^- monocation $\mathbf{1}^+$ (next section).

Catalytic Isomerization Demonstrated at Electrode Surfaces. Conversion of **1** to **2** at an electrode surface may be qualitatively demonstrated by the following experiment on a solution of **1**. The electrode is first set at a rest potential at least 500 mV negative of $E^{\mathbf{1}}_{1/2}$ for 30 s, then scanned *negatively* (Figure 3, scan a). The rest potential is chosen to be so much negative of the oxidation of **1** that *no* $\mathbf{1}^+$ is formed, that is, the concentrations at the electrode surface are the same as those in the bulk of solution. The cathodic peak heights at *ca.* −1.9 and −1.7 V are proportional to the concentrations of isomers **1** and **2**, respectively, near the electrode because (i) the two neutral isomers give one-electron reduction waves at these potentials (*vide infra*) and (ii) the isomers do not interconvert on the CV time scale in either the 48 e^- or 49 e^- complexes. This experiment is repeated for gradually more positive rest potentials (Figure 3, scans b−d). In doing so, some enrichment of **2** at the expense of **1** is seen in scans that start closer to the oxidation of isomer **1** (in scan d the small peak at *ca.* −1.3 V is indicative of Cp_2Co^+ formed by the partial decomposition of $\mathbf{1}^+$ or $\mathbf{2}^+$). This experimental approach was used earlier to estimate a formal potential for an isomer of $Cp_3Rh_3(CO)_3$ that could not be detected directly.[15] In the present case, however, the $E_{1/2}$ values of both isomers are accessible from CV scans of their anodic processes, and it is to that data that we now turn.

Measurement of Isomerization Rate: 47-Electron Cation $\mathbf{1}^+ \rightarrow \mathbf{2}^+$. The anodic responses for **1** and **2** depend on the ratio k^+_f/a, where k^+_f is the rate of the isomerization of $\mathbf{1}^+$ to $\mathbf{2}^+$ (eq 2) and a is a parameter proportional to scan rate ($a = \nu F/RT$). Small values of k^+_f/a (slow isomerization/fast scan limit) lead to dominance for the anodic wave of **1** since there

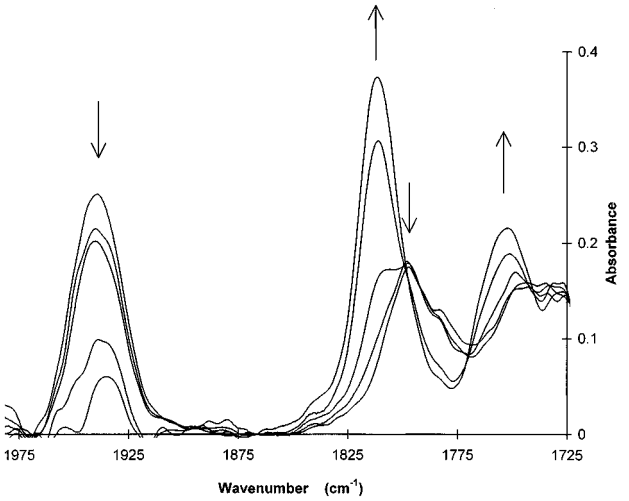

Figure 2. IR spectra in the CO region recorded during the anodic catalytic conversion of 1.0 mM **1** (in CH_2Cl_2) to **2** at a Pt gauze electrode ($E_{appl} = -0.6$ V) at ambient temperature. Spectra were obtained by use of a fiber-optic IR probe as described in ref 25.

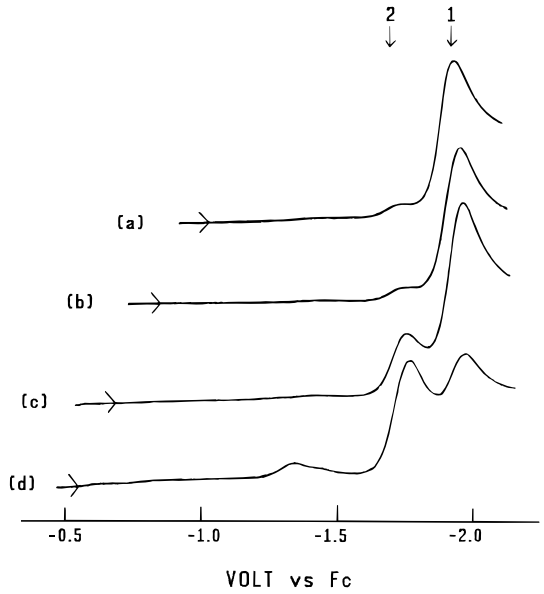

Figure 3. CV scans ($\nu = 10$ V/s) of the cathodic waves observed when a 0.64 mM solution of **1** in CH_2Cl_2 is held at increasingly positive potentials (from a to d) in order to initiate the electrocatalytic conversion of **1** to **2**. The observed waves correspond to the 48 e^-/49 e^- couples of **1** and **2**.

is insufficient time for conversion of $\mathbf{1}^+$ to $\mathbf{2}^+$ during the scan. In the opposite extreme, large values of k^+_f/a (fast isomerization/slow scan limit) give a dominant response for isomer **2** since $\mathbf{1}^+$ has time for isomerization to $\mathbf{2}^+$ (and subsequent reduction to **2**) during the scan. Given sufficient time, the conversion of **1** to **2** is virtually quantitative. In between the two extremes is a kinetic range in which changes in the relative heights of **1** and **2** may be used to determine the value of k^+_f.

For quantitative voltammetric analysis, CH_2Cl_2 was chosen over THF owing to the lower ohmic effects of the former, especially at subambient temperatures. At ambient temperatures scan rates in excess of 100 V/s were necessary to achieve dominance of peak A (for solutions of **1**). At these scan rates ohmic effects were appreciable, so quantitative fits were restricted to scan rates below about 5 V/s. Concentration effects were probed since the ETC isomerization might also occur (in addition to the heterogeneous route of eqs 1−3) through the homogeneous cross reaction of eq 5:

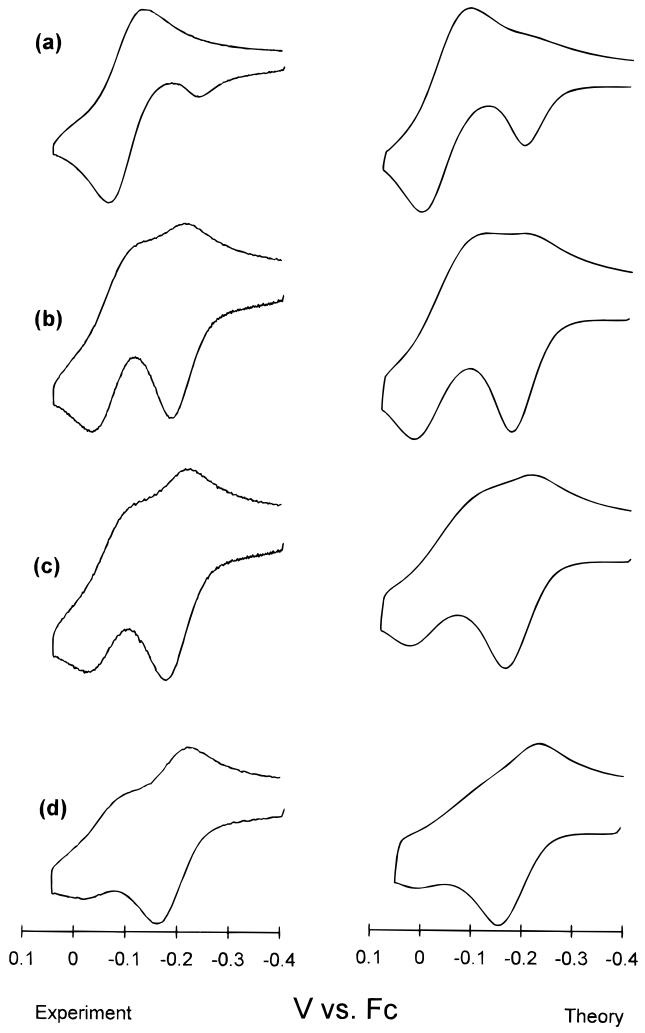

Figure 4. Experimental (left) and digitially simulated (right) CV responses of 0.21 mM **1** in CH_2Cl_2 at 228 K. Scan rates are (a) 0.05, (b) 0.20, (c) 0.40, and (d) 1.0 V/s. Simulation parameters given in Table 3.

$$\mathbf{1} + \mathbf{2}^+ \rightleftharpoons \mathbf{2} + \mathbf{1}^+ \qquad (5)$$

Concentrations between 0.2 mM and *ca.* 1.5 mM did not give appreciable differences in the anodic peak heights for **1** and **2**, arguing against eq 5 playing an important role in the electrode reaction layer (eq 5 must, however, be the dominant mechanistic route in the bulk electrolysis). Unusual peak broadening was observed in the cathodic return wave of **2** when CH_2Cl_2 was the solvent and concentrations were above 1 mM. Since the reason for this is not presently understood, and wanting to minimize any contribution from the cross-reaction of eq 5, we chose the lowest concentration data (0.21 mM) for quantitative analysis, in spite of the less favorable ratio of analyte-to-background currents.

Typical of the general trends, at 237 K over a range of ν from 0.025 to 3.2 V/s the ratio of wave A (**1**) to wave B (**2**) goes about from 0.4 to 5. In the data set at 228 K (Figure 4), at low ν the cathodic return peak for wave B is resolved; at high ν that of A is resolved. At intermediate ν the overlap of the two cathodic contributions is apparently caused by a slower heterogeneous charge transfer reaction for **2** compared to **1** [k_s(**2**) = 0.005 cm/s and k_s(**1**) = 0.06 cm/s at 228 K)]. The parameters $E^{\mathbf{1}}_{1/2}$ and k_s(**1**) were available from the high-scan rate data; $E^{\mathbf{2}}_{1/2}$ and k_s(**2**) were obtained from the low-scan rate data. In the simulations (Figure 4) the value of K^+_{eq} (eq 4) was set at 100 (i.e, isomer **2** is highly thermodynamically

Table 1. Formal Potentials of Clusters $Cp^*IrCp_2Co_2(CO)(\mu\text{-}CO)_2$ (**1**) and $Cp^*IrCp_2Co_2(\mu\text{-}CO)_3$ (**2**) vs Ferrocene/Ferrocenium

couple	solvent	$E_{1/2}$ (V)[a]
	Oxidations	
$\mathbf{1}/\mathbf{1}^+$	CH_2Cl_2 or THF	−0.44
$\mathbf{2}/\mathbf{2}^+$	CH_2Cl_2 or THF	−0.30
	Reductions	
$\mathbf{1}/\mathbf{1}^-$	THF	−1.88
$\mathbf{1}^-/\mathbf{1}^{2-}$	THF	−2.82[b]
$\mathbf{2}/\mathbf{2}^-$	THF	−1.64

[a] Measured from the average of E_{pc} and E_{pa}. [b] Chemically irreversible (E_{pc} at $\nu = 0.2$ V/s reported).

Table 2. Rate and Equilibrium Constants Determined in This Study

Isomerization of 47e Monocations					
process	constant	defined	temp, K	value, s^{-1}	method
$\mathbf{1}^+ \rightarrow \mathbf{2}^+$	k^+_f	eq 2	298	400	CV[a]
	k^+_f		293	300	CV
	k^+_f		293	400	SW[a]
	k^+_f		237	8	CV

Isomerization of 48e Neutral Clusters $\mathbf{1} \rightarrow \mathbf{2}$ (determined by ^1H NMR)		
temp, K	$K^0_{eq}([\mathbf{2}]/[\mathbf{1}])$[b]	$k^0_f(\mathbf{1}\rightarrow\mathbf{2})$[b], s^{-1}
345	1.59	5.4×10^{-4}
340	1.79	2.7×10^{-4}
330	2.38	8.4×10^{-5}
320	c	2.3×10^{-5}
315	4.00	1.5×10^{-5}
297	7.14	$[1 \times 10^{-6}]$[d]
237	c	$[1 \times 10^{-11}]$[d]

Decomposition of 47e Monocation $\mathbf{2}^+$					
process	constant	defined	temp	value, s^{-1}	method
$\mathbf{2}^+ \rightarrow$ dec	k_c	eq 4	ambient	0.30	CV

[a] CV = cyclic voltammetry; SW = square wave voltammetry. [b] K^0_f and k^0_f defined in eq 7. [c] Not determined. [d] Value extrapolated from temperature dependence.

favored in the monocations) although we have no independent measure of this quantity. The general features of the experimental data, and especially the ratios of anodic peak currents, were adequately reproduced with $k^+_f = 8\ s^{-1}$ at 237 K. Changes of greater than *ca.* 50 % in k^+_f produced visually inferior fits. Virtually identical data and theoretical fits were obtained from a second experiment on a different day in which the concentration was 0.30 mM.

Fitting the ambient temperature CV data (in Supporting Information) Figure 1 required an additional rate constant describing the decomposition of $\mathbf{2}^+$ (k_c in eq 4). This value was obtained independently from data at 298 K in THF (concentration = 1.2 mM). From the ratio of i_{rev}/i_{fwd} at various ν,[28] and assuming a first-order decomposition reaction, a value of $k_c = 0.30\ s^{-1}$ (± 0.08) was determined and used in simulations of the ambient temperature data. The half-life of *ca.* 2 s for $\mathbf{2}^+$ at ambient temperatures is consistent with bulk electrolysis results (*next section*). Simulations of separate experiments were consistent with $k^+_f = 300\ s^{-1}$ at 293 K (Figure 1 in the Supporting Information) and $k^+_f = 400\ s^{-1}$ at 298 K. Table 2 summarizes the chemical rate constant data measured for these systems.

Square-wave voltammetry was also used to determine the isomerization rate constant k^+_f by simulating the relative peak heights of the two anodic waves at 293 K in the lowest concentration experiment. Rate constants of 300−400 s^{-1} gave adequate agreement with experimental results although systematic work was not done to establish error limits. The square-wave and CV rate constant determinations are in excellent agreement. Figure 5 shows typical square-wave data and simulations (rate constants in Table 2, simulation parameters in Table 3).

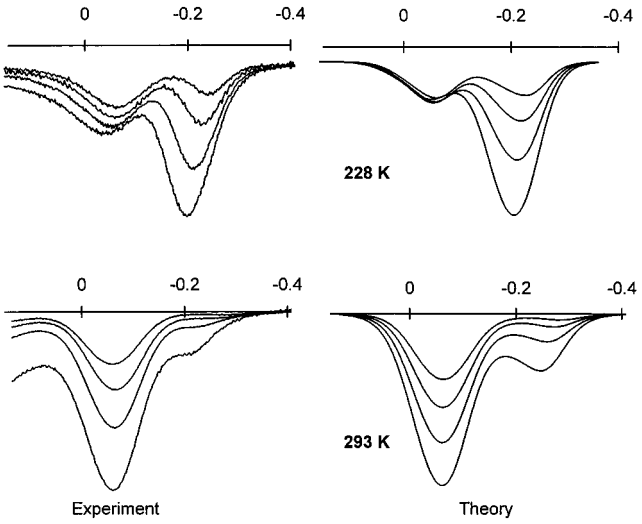

Figure 5. Experimental (left) and digitally simulated (right) square-wave voltammograms of 0.21 mM **1** in CH_2Cl_2 at $T = 228$ (top) and 293 K (bottom). Scans recorded with 2 mV pulse width and 50 mV pulse height at frequencies of 25, 50, 100, and 200 Hz.

Table 3. Parameters Used for Simulation of Cyclic Voltammetry and Square Wave Voltammetry Experiments

reaction or couple	$E_{1/2}$, V	k_s, $cm \cdot s^{-1}$	α	k^+_f, s^{-1}	k_c, s^{-1}	other
(i) 293 K, Cyclic Voltammetry and Square-Wave Voltammetry						
$\mathbf{1}/\mathbf{1}^+$	−0.44	0.3	0.5			R_u, C_{dl}[a]
$\mathbf{2}/\mathbf{2}^+$	−0.30	0.05	0.3			
$\mathbf{1}^+ \rightarrow \mathbf{2}^+$				300		$K^+_{eq} = 100$
$\mathbf{2}^+ \rightarrow$ dec					0.30	
(ii) 237 K, Cyclic Voltammetry						
$\mathbf{1}/\mathbf{1}^+$	−0.44	0.06	0.5			R_u, C_{dl}[b]
$\mathbf{2}/\mathbf{2}^+$	−0.30	0.005	0.3			
$\mathbf{1}^+ \rightarrow \mathbf{2}^+$				8		$K^+_{eq} = 100$

[a] $R_u = 40\ \Omega$, $C_{dl} = 1\ \mu F$. [b] $R_u = 500\ \Omega$, $C_{dl} = 5\ \mu F$.

Ultimate Fragmentation of 47-Electron Cluster $\mathbf{2}^+$. When **2** is anodically electrolyzed at a Pt basket in CH_2Cl_2 ($E_{appl} = 0$ V, positive of the couple $\mathbf{2}/\mathbf{2}^+$) the cluster fragments into mononuclear components. The only major CO-containing signals (Figure 2 in the Supporting Information; fiber-optic probe method) may be assigned to $CpCo(CO)_2$ ($\nu_{CO} = 2022$ and 1959 cm^{-1}) and $Cp^*Ir(CO)_2$ ($\nu_{CO} = 2012$ and 1936 cm^{-1}); bands at 1812 and 1749 cm^{-1} are assigned to **2** (arising either from incomplete electrolysis or regeneration from $\mathbf{2}^+$). A small band at 1843 cm^{-1} is unassigned. No significant absorbances were detected in the CO-bridging region arising possibly from the dinuclear complexes $Cp_2Co_2(\mu\text{-}CO)_2$[29] or $Cp^*IrCpCo(\mu\text{-}CO)_2$.[30] The product solution contained a significant electrochemical wave for the reduction of cobaltocenium ion at −1.33 V.[31] Eventually, therefore, the electron-deficient cluster $\mathbf{2}^+$ fragments to at least the three products given in eq 6:

$$\mathbf{2}^+ \rightarrow Cp_2Co^+ + CpCo(CO)_2 + Cp^*Ir(CO)_2 + ? \quad (6)$$

Isomerization of 48-Electron Neutral Clusters $\mathbf{1} \rightleftharpoons \mathbf{2}$ Studied by NMR. The neutral cluster **1** rearranges over a

(28) Nicholson, R. S.; Shain, I. *Anal. Chem.* **1964**, *36*, 706.

(29) $Cp_2Co_2(CO)_2$: Cotton, F. A.; Piper, T. S.; Wilkinson, G. *J. Inorg. Nucl. Chem.* **1955**, *1*, 165.

(30) $Cp^*IrCo(CO)_2$: Kang, J. W.; Moseley, K.; Maitlis, P. M. *J. Am. Chem. Soc.* **1969**, *91*, 5970.

(31) Connelly, N. G.; Geiger, W. E. *Chem. Rev.* **1996**, *96*, 877.

period of several days in solution at ambient temperatures, resulting in an equilibrium mixture of **1** and the all-CO-bridging isomer **2**. The relative concentrations of each were followed by integrations of their Cp ^{1}H NMR signals. Typically about 10% of the starting material was lost to decomposition in the course of the isomerization from isomer **1** to isomer **2**. The intensities of isomers **1** and **2**, normalized for the amount of material lost to decomposition, fit well with a first-order kinetic scheme (data at 315 K in Figure 3 in the Supporting Information). Repeated at temperatures over the range 315 to 345 K, these measurements yielded the equilibrium and rate constants in Table 2. Note that K^0_{eq} and k^0_f are defined as in eq 7:

$$\mathbf{1} \underset{k^0_b}{\overset{k^0_f}{\rightleftharpoons}} \mathbf{2} \qquad K^0_{eq} = [\mathbf{2}]/[\mathbf{1}] \tag{7}$$

The isomerization rate k^0_f, which approaches 10^{-5} s^{-1} at 315 K ($\approx 10^{-6}$ s^{-1} at 298 K), is almost a *billionfold* lower than that, k^+_f, of the 47 e$^-$ monocation at a similar temperature. Also of note is that the changes in K^0_{eq} with temperature establish that the all-CO-bridging complex **2** is the thermodynamically favored isomer in the 48 e$^-$ clusters.

The data in Table 2 were used to obtain free energy differences between the two neutral isomers and the free energy of activation of the isomerization process. A plot of ln K^0_{eq} *vs.* $1/T$ gave $\Delta H = -28$ kJ/mol ($\Delta G^o_{298} = -4.8$ kJ/mol). The activation barrier to isomerization of the 48-electron cluster **1** was obtained from a plot of $\ln(k^o_f \cdot h/kT)$ *vs.* $1/T$), giving $\Delta H^‡ = 107(4)$ kJ/mol and $\Delta S^‡ = 2(11)$ J·mol^{-1}·K^{-1}. The entropy term is close to zero as expected for an intramolecular reaction. From these values a free energy of activation at 298 K of $\Delta G^‡ = 107$ kJ/mol is calculated. These data were used to calculate isomerization rate constants at 297 and 237 K (Table 2) which were used to compare to the rate constants of the 47 e$^-$ and 49 e$^-$ complexes.

Cathodic Reduction of 1. A CV scan of a solution containing *ca.* 90% **1** and 10% **2** (IR, NMR) between −1.1 and −3.1 V is shown in Figure 6. The wave at $E_{1/2} = -1.88$ V (having partial chemical reversibility) (Figure 6, top; $\nu = 0.2$ V/s) is assigned to the one-electron reduction of **1** (eq 8), whereas the small "prewave" at $E_{1/2} = -1.64$ V arises from **2**. Isomer **2**, with its all-CO-bridging arrangement,

$$\mathbf{1} \overset{e^-}{\rightleftharpoons} \mathbf{1}^- \overset{e^-}{\rightleftharpoons} \mathbf{1}^{2-} \rightarrow \text{unknown product} \tag{8}$$

is easier to reduce by 240 mV compared to isomer **1** which has one terminal CO and two edge-bridging COs. The higher electron affinity implied for the all-bridging CO complex is very similar to that reported earlier (210 mV) for C_{3v}-$Cp_3Rh_3(\mu\text{-CO})_3$ ($E_{1/2} = -1.01$ V) compared to C_s-$Cp_3Rh_3(CO)(\mu\text{-CO})_2$ ($E_{1/2} = -1.22$ V).[15]

Assignments of the waves at yet more negative potentials are unclear. By analogy with the isomeric pair C_{3v}-$Cp_3Rh_3(CO)_3$ and C_s-$Cp_3Rh_3(CO)_3$,[15] one expects that **1** and **2** will have second reductions which are very close in potential. The reversibility of the features between −2.8 and −3.0 V varies with scan rate (Figure 6, bottom). Interpreting conservatively, the CV data are insufficient to draw *mechanistic* conclusions about isomeric interconversions in the 50 e$^-$ dianions. The **1**/**1**$^-$ couple (−1.88 V) showed a small deviation from chemical reversibility that suggested a half-life of ≥10 s for **1**$^-$ at ambient temperatures. Noting the possibility that the follow-up reaction of **1**$^-$ might be its isomerization to **2**$^-$, the bulk reduction of **1** was investigated in order to probe the fate of **1**$^-$ over a longer time period.

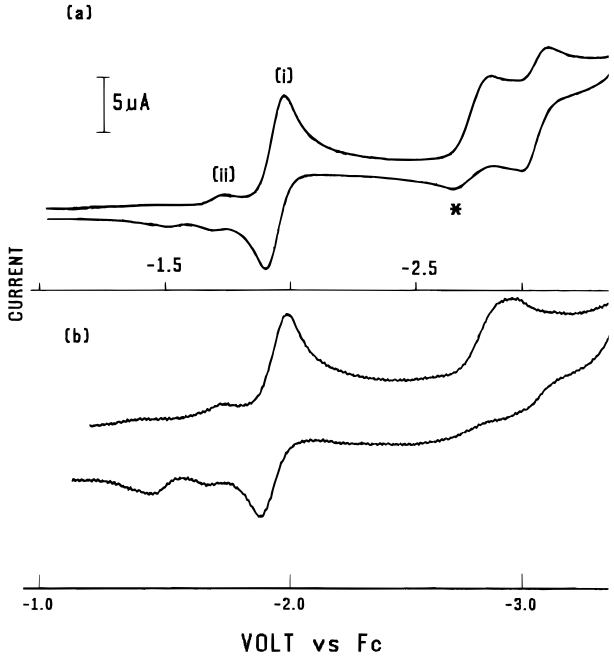

Figure 6. CV scans of reduction waves of 0.6 mM **1** in THF at (a) $\nu = 0.2$ and (b) 10 V/s (Pt electrode, ambient temperature). The asterisk denotes a feature that was absent unless the scan was carried out past the most negative wave at −3 V.

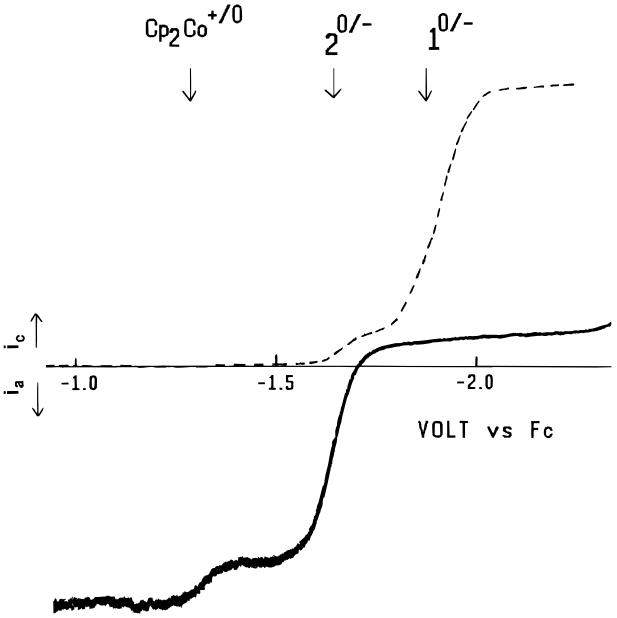

Figure 7. Steady-state voltammograms recorded at a rotating Pt electrode before (dashed line) and after (solid line) the exhaustive reduction of a solution of 1.0 mM **1** (with about 5% **2**) at −2 V showing conversion from neutral **1** to anionic **2**.

In a bulk cathodic reduction of **1** at $E_{appl} = -2.0$ V the waves of **1** were replaced by that of **2** ($E_{1/2} = -1.64$ V) as the major product, the yield of the latter being 40−80% in five replicates (average $n_{app} = 1.05$ e$^-$). Rotating Pt electrode voltammetry showed that between half and all of isomer **2** was present as the anion, the balance being neutral **2**. A small amount of cobaltocene also formed (Figure 7). When electrolyzed solutions containing the anion **2**$^-$ were monitored for an additional 30 min, no further decomposition was observed. The fragmentation of the anion signaled by the appearance of Cp_2Co seems, therefore, to arise from the anion of **1** rather than that of **2**. The anion **2**$^-$ is stable when protected from air. After re-oxidation

of the reduced solutions at $E_{appl} = -1.1$ V, IR spectra confirmed the presence of **2** and the absence of **1**.

Reduction of **1** by one electron gives, therefore, moderate yields of the all-CO-bridging isomer **2**, the conversion being complete within the time scale (*ca.* 15 min) of the bulk electrolysis. Whether the isomerization occurs directly, by intramolecular rearrangement of the 49 e$^-$ anion or indirectly, by fragmentation of the anion followed by reassembly of the cluster in a kinetically favored form, cannot be answered by these data alone. The limits on the rate of the isomerization, k^-_f, of the 49 e$^-$ anion can, however, be set between 10^{-1} and 10^{-3} s^{-1}. The fact that ESR spectra measured after brief contacts with alkali metal (next section) do not show features arising from **1**$^-$ implies that k^-_f lies closer to the faster of these two limits, namely *ca.* 10^{-1} s^{-1}.

It should be noted that the isomerization of the 49 e$^-$ anion **1**$^-$ is stoichiometric (1 faraday/equiv) rather than catalytic (as in the 47 e$^-$ cation **1**$^+$) in the number of electrons required because the reduction **1**/**1**$^-$ is *negative* of the reduction **2**/**2**$^-$; reoxidation to the neutral complex **2** cannot occur at the potential necessary to produce **1**$^-$.

ESR Spectra of the 49-Electron Anion [Cp*IrCp$_2$Co$_2$(CO)$_3$]$^-$ (2$^-$). Potassium mirror reduction of **1** (containing 10% **2**) in THF or Me-THF (213 K, 1 min contact time, high vacuum) produced an off-green solution having a fluid solution ESR spectrum showing hyperfine interaction with two equivalent Co nuclei (Figure 4 in the Supporting Information), $\langle g \rangle = 2.028$, $\langle \mathrm{Co} \rangle = 43 \times 10^{-4}$ cm^{-1}. At 77 K the spectrum had the appearance of an axial or nearly-axial system with g_1 ($\approx g_{||}$) = 2.066, A_1(Co) ($\approx A_{||} = 89 \times 10^{-4}$ cm^{-1}), and the other (smaller) hyperfine components being too poorly resolved for extraction of accurate values.[32] Allowing this solution to stand overnight under vacuum resulted in no noticeable changes in the ESR spectrum. When exposed to air, however, the color changed immediately to the dark red of **2**; voltammetric analysis of the red solution showed only the waves of **2** and (as a minor component) Cp$_2$Co$^+$. The ESR spectrum is assigned to **2**$^-$ rather than **1**$^-$ on the basis of these observations and on the known stablity of **2**$^-$ established previously in bulk electrolyses.

The ESR parameters assigned to **2**$^-$ are readily interpreted through comparison with results on a number of isoelectronic trimetallic clusters containing two or three Co atoms.[33−36] Isotropic Co hyperfine splittings of *ca.* 30×10^{-4} cm^{-1}, with a maximum of *ca.* 70×10^{-4} cm^{-1} (along the low-field *g* value, g_1) have been reported for systems such as Co$_3$(CO)$_9$(μ-S),[33] Co$_3$(CO)$_9$(μ-PR),[34] [Co$_3$(CO)$_9$(μ-CR)]$^-$,[35] and [FeCo$_2$(CO)$_9$(μ-S)]$^-$.[35] References 33 and 35 give quantitative descriptions of the bonding in these clusters and the spin-density distributions in the 49 e$^-$ species. The SOMO is in the trimetallic plane and is antibonding with respect to the metal−metal bonds. Approximately 0.25 e$^-$ resides on the Co atoms in both [Co$_3$(CO)$_9$(μ-CR)]$^-$ and [FeCo$_2$(CO)$_9$(μ-S)]$^-$ according to the analysis of Rieger *et al.*[35] Given that the isotropic Co hyperfine splitting is likely to be proportional to the Co spin density in these systems,[35,37] the parameters measured for [Cp*IrCp$_2$Co$_2$(CO)$_3$]$^-$ suggest that the SOMO is considerably more localized on the two Co atoms than on Ir, with *ca.* 0.35−0.40 e$^-$ on each of the former. Assuming that about 0.2 e$^-$ is distributed to the CO and C$_5$R$_5$ ligands[35] leaves very little spin for the Ir atom. The SOMO of this system appears localized, therefore, on the dicobalt section of the molecule.[38]

Discussion

Thermodynamic Preferences. The all-CO-bridging complex appears to be the thermodynamically-prefered isomer in all three cluster oxidation states. Determination of the actual equilibrium constant was possible only in the case of the neutral 48 e$^-$ cluster (e.g., $K^0_{eq} \approx 7$ at 297 K). We can be sure, however, that K_{eq} increases for the 47 e$^-$ cation because a value less than about 10 for K^+_{eq} would have been detected when comparing experimental and simulated CVs. An estimate of K^-_{eq} for the 49 e$^-$ anion is not possible from the present data.

The potentials of the two redox processes **2**/**2**$^-$ and **2**/**2**$^+$ are both positive of their counterparts for **1** (by 240 and 140 mV, respectively), consistent with the greater abililty of bridging carbonyls to accept metal dπ electron density.[39,40] The reduction data compare well with the difference measured for the analogous trirhodium clusters **3** and **4** (210 mV).[15]

Kinetics of Isomerizations. If the isomerization rate of the 49 e$^-$ system is taken as about 10^{-2} s^{-1} (the actual rate is between 10^{-1} and 10^{-3} s^{-1}), then relative rates (at 298 K) of 1:10^4:10^8 may be assigned to the isomerization of the 48 e$^-$:49 e$^-$:47 e$^-$ species. We now turn to considerations of bonding in these clusters in order to rationalize these large rate differences.

Cluster Redox Orbitals. A number of calculations relevant to the structure and bonding of these trinuclear clusters have been published. Braga and co-workers[19] have addressed the preferences for bridging- *vs* terminal-COs in *homo*trinuclear complexes of the type Cp$_3$M$_3$(CO)$_3$ (M = Co, Rh, Ir). Although their conclusions about the favored isomers in the 48 e$^-$ complexes are not directly applicable to our odd-electron species, we will make use of some of their general principles in the following discussion.

Of perhaps more direct relevance are calculations which characterize the orbital makeup of the HOMO and the LUMO of these systems and allow a glimpse at the effect that altering the electron count might have on the molecular structure. Because CpM is isolobal with (CO)$_3$M it is appropriate to focus on calculations of 48 e$^-$ clusters[39] of the type M$_3$(CO)$_{12}$, which have been the subject of a number of studies.[41−45] There is general agreement that the HOMO is bonding and the LUMO

(32) Approximating the spectrum as axial allows an estimate of $A_\perp$ (i.e., the average of A_2, A_3) as 22.5×10^{-4} cm^{-1} and $g_\perp$ (the average of g_2 and g_3) as 2.009.

(33) Strouse, C. E.; Dahl, L. F. *Discuss. Faraday Soc.* **1969**, *47*, 83.

(34) Beurich, H.; Madach, T.; Richter, F.; Vahrenkamp, H. *Angew. Chem., Int. Ed. Engl.* **1979**, *18*, 690.

(35) Peake, B. M.; Rieger, P. H.; Robinson, B. H.; Simpson, J. *Inorg. Chem.* **1981**, *20*, 2540.

(36) Peake, B. M.; Rieger, P. H.; Robinson, B. H.; Simpson, J. *J. Am. Chem. Soc.* **1980**, *102*, 156.

(37) Mao, F.; Tyler, D. R.; Rieger, A. L.; Rieger, P. H. *J. Chem. Soc., Faraday Trans.* **1991**, *87*, 3113.

(38) The hyperfine splittings measured for the radical assigned as **2**$^-$ are very close to those reported for the dinuclear anion [Cp$_2$Co$_2$(μ-CO)$_2$]$^-$. It is important, therefore, to note that the isotropic *g*-value of the radical reported in the present paper ($\langle g \rangle = 2.028$) is sufficiently different from that of the family of [(C$_5$H$_4$R)$_2$Co$_2$(μ-CO)$_2$]$^-$ ($\langle g \rangle = 2.09 \pm 0.01$ [(a) Schore, N. E.; Ilenda, C. S.; Bergman, R. G. *J. Am. Chem. Soc.* **1977**, *99*, 1781. (b) Schore, N. E. *J. Organomet. Chem.* **1979**, *173*, 301. (c) Cirjack, L. M.; Ginsburg, R. E.; Dahl, L. F. *Inorg. Chem.* **1982**, *21*, 940. (d) Symons, M. C. R.; Bratt, S. W. *J. Chem. Soc., Dalton Trans.* **1979**, 1739. (e) Geiger, W. E.; Gennett, T.; McVicar, W. K.; Herrmann, W. A. *Organometallics* **1987**, *6*, 1634]) so as to exclude the possibility of their mutual misidentification.

(39) (a) Chini, P. *Pure Appl. Chem.* **1970**, *23*, 489. (b) Shriver, D. F. *Chem. Br.* **1972**, *8*, 419. (c) Chini, P. *Inorg. Chim. Acta Rev.* **1968**, *2*, 31. (d) Albano, V. G.; Ciani, G.; Martinengo, S. *J. Organomet. Chem.* **1974**, *78*, 265.

(40) (a) Kristoff, J. S.; Shriver, D. F. *Inorg. Chem.* **1974**, *13*, 499. (b) Cotton, F. A.; Troup, J. M. *J. Am. Chem. Soc.* **1974**, *96*, 1233. (c) Wade, K. In *Transition Metal Clusters*; Johnson, B. F. G., Ed.; J. Wiley and Sons: Chichester, 1980; p 206.

(41) Lauher, J. W. *J. Am. Chem. Soc.* **1978**, *100*, 5305.

(42) Schilling, B. E. R.; Hoffman, R. *J. Am. Chem. Soc.* **1979**, *101*, 3456.

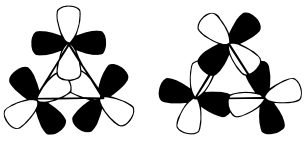

Figure 8. Representation of the proposed metal contributions to the HOMO and LUMO orbitals of 48 e$^-$ $Cp_3M_3(CO)_3$ based on results in refs 42 and 43.

antibonding, with respect to the trimetal core. Figure 8 sketches the metal contributions of the two orbitals in question. The HOMO contains considerable carbonyl character and may be more highly delocalized between metals and ligands than previously thought.[43]

On the basis of the M_3-antibonding LUMO, 49 e$^-$ anions of the type $[Cp_3M_3(CO)_{12}]^-$ are expected to have elongated M−M bonds. This has been confirmed in structural studies of trimetallic clusters containing from 48 to 50 electrons.[46] In the extreme, especially for two-electron reductions, there may be scission of a specific metal−metal bond such as implied for the reduction of $Ru_3(CO)_{12}$[47] and confirmed in the reduction of $Fe_3(CO)_9(\mu\text{-PR})_2$[48] and other clusters.[49] Since calculations show that weaker M−M bonds favor bridging over terminal carbonyls,[19] only *elongation* of the M−M bonds, rather than scission, in the transition state, is required to explain the enhanced rate of formation of the all-bridging isomer in the 49 e$^-$ complex $[Cp^*IrCp_2Co(CO)_3]^-$.

The situation is less clear when considering how the HOMO influences the structure of the 47 e$^-$ oxidation product. The characterization of the HOMO as a trimetal-centered bonding orbital[42] suggests that removal of an electron will increase the metal−metal distance, favoring bridging COs; the reduced electron density in the monocation, however, argues for the terminal CO isomer. Yet another effect besides charge and M−M distance may be important. A higher level calculation on $Ru_3(CO)_{12}$ indicates that there is considerable admixture of M−CO π bonding in the HOMO.[43] Oxidation would therefore be expected to lead to weaker M−CO bonds as well as longer M−M bonds. The former may influence the isomerization activation barrier but a more in-depth theoretical study would be necessary to investigate this. The weaker M−CO bonding raises the question of possible CO lability in the monocation. Although we cannot rule this out, it seems unlikely to be important in the isomerization process in view of the observed quantitative conversion from **1**$^+$ to **2**$^+$ (loss of CO may, however, trigger the decomposition of **2**$^+$, eq 6).

Summary

The all-CO-bridging form of $Cp^*IrCp_2Co_2(CO)_3$ appears to be the more stable isomer in each of three different cluster oxidation states. Enormous enhancements of the isomerization rate are observed, however, in the odd-electron complexes. Labeling the cluster by its electron count, k_{isom} increases in the order 48 e$^-$ ≪ 49 e$^-$ ≪ 47 e$^-$ with the relative rates 1:≈10^4:10^8. The fact that very fast electron-transfer-catalyzed isomerization has been observed in this system as well as a trirhodium analogue[15] means that trinuclear clusters (and perhaps other clusters) may be particularly prone to facile ligand isomerizations triggered by adventitious oxidants. If these complexes are viewed as models for carbon monoxide adsorbed onto metal surfaces, the implication is that terminal-to-bridging CO rearrangements may be very rapid on these surfaces if they contain odd-electron sites.

Acknowledgment. This work was supported at the University of Vermont by grants from the Petroleum Research Fund (PRF) (28321-AC) and the National Science Foundation (CHE94-16611) and at the University of Tennessee by a PRF grant (29106-AC).

Supporting Information Available: Figures giving the experimental and digitally simulated CV responses of **1** in CH_2Cl_2, IR spectrum after exhaustive anodic electrolysis of **1** in CH_2Cl_2, integrated ^{1}H-NMR resonances of **1** and **2**, and fluid solution ESR spectrum of the reduction product of 1 in THF after brief contact with K at 213 K (5 pages). See any current masthead page for ordering and Internet access instructions.

JA963476K

(43) (a) Trogler, W. C. *Acc. Chem. Res.* **1990**, *23*, 239. (b) Delley, B.; Manning, M. C.; Ellis, D. E.; Berkowitz, J.; Trogler, W. C. *Inorg. Chem.* **1982**, *21*, 2247.

(44) Tyler, D. R.; Levanson, R. A.; Gray, H. B. *J. Am. Chem. Soc.* **1978**, *100*, 7888.

(45) Mingos, D. M. P.; Wales, D. J., Eds. *Introduction to Cluster Chemistry*; Prentice Hall: Englewood Cliffs, 1990; p 82 and references therein.

(46) For leading references see: Byers, L. R.; Uchtman, V. A.; Dahl, L. F. *J. Am. Chem. Soc.* **1981**, *103*, 1942.

(47) Cyr, J. C.; DeGray, J. A.; Gosser, D. K.; Lee, E. S.; Rieger, P. H. *Organometallics* **1985**, *4*, 950.

(48) Koide, Y.; Bautista, M. T.; White, P. S.; Schauer, C. K. *Inorg. Chem.* **1992**, *31*, 3690.

(49) Venturelli, A.; Rauchfuss, T. B. *J. Am. Chem. Soc.* **1994**, *116*, 4824.